hep-ph/0610344
KEK–TH–1106
October 2006

Lepton Flavour Violating τ Decays in the Left-Right Symmetric Model

A.G. Akeroyd[1,3,4*], Mayumi Aoki[1†] and Yasuhiro Okada[1,2‡]

1: Theory Group, KEK, 1-1 Oho, Tsukuba, Ibaraki, 305-0801 Japan

2: The Graduate University for Advanced Studies (Sokendai), 1-1 Oho, Tsukuba, Ibaraki, 305-0801 Japan

3: Department of Physics, National Cheng Kung University, Tainan, 701 Taiwan

4: National Center for Theoretical Sciences, Taiwan

Abstract

The Left-Right symmetric extension of the Standard Model with Higgs isospin triplets can provide neutrino masses via a TeV scale seesaw mechanism. The doubly charged Higgs bosons $H_L^{\pm\pm}$ and $H_R^{\pm\pm}$ induce lepton flavour violating decays $\tau^\pm \to lll$ at tree-level via a coupling which is related to the Maki-Nakagawa-Sakata matrix ($V_{\rm MNS}$). We study the magnitude and correlation of $\tau^\pm \to lll$ and $\mu \to e\gamma$ with specific assumptions for the origin of the large mixing in $V_{\rm MNS}$ while respecting the stringent bound for $\mu \to eee$. It is also shown that an angular asymmetry for $\tau^\pm \to lll$ is sensitive to the relative strength of the $H_L^{\pm\pm}$ and $H_R^{\pm\pm}$ mediated contributions and provides a means of distinguishing models with doubly charged Higgs bosons.

PACS index: 13.35.-r, 14.60.Pq, 14.80.Cp
Keywords : Higgs boson, Neutrino mass and mixing, Lepton flavour violation

*akeroyd@mail.ncku.edu.tw
†mayumi.aoki@kek.jp
‡yasuhiro.okada@kek.jp

1 Introduction

In recent years there has been increasing evidence that neutrinos oscillate and possess a small mass below the eV scale [1]. This revelation necessitates physics beyond the Standard Model (SM), which could manifest itself at the CERN Large Hadron Collider (LHC) and/or in low energy experiments which search for lepton flavour violation (LFV) [2]. Consequently, models of neutrino mass generation which can be probed at present and forthcoming experiments are of great phenomenological interest.

Massive neutrinos may be accommodated by adding a $SU(2)_L$ singlet ("sterile") right-handed neutrino ν_R to the SM Lagrangian together with the corresponding Dirac mass term. In order to obtain masses of the eV scale, the Yukawa coupling of the neutrinos to the SM Higgs boson would need to be at least 6 orders of magnitude smaller than the electron Yukawa coupling. Moreover, there would be no observable phenomenological consequences aside from neutrino oscillations. More appealing frameworks for neutrino mass generation can be found if neutrinos are of the Majorana type. The celebrated seesaw mechanism [3] ascribes the smallness of the neutrino mass to the large scale of the unobserved *heavy* right-handed neutrinos (N_R). Dirac mass terms of the order of the top quark mass would require $N_R \sim 10^{14}$ GeV, a scale which is far beyond the reach of any envisioned collider. Reducing the scale of N_R to the order of a few TeV would require Dirac mass terms of the order of MeV, which constitutes a mild fine-tuning with respect to magnitude of the charged lepton masses. However, such a choice would permit the mechanism to be probed at future high-energy colliders. This "low energy seesaw mechanism" may be implemented in Left-Right (LR) symmetric models [4] with Higgs triplet representations [5], in which the mass matrix for N_R is given by the product of a new Yukawa coupling h_{ij} and a triplet vacuum expectation value (vev) v_R. The mass scale of the other new particles in the model (e.g. the new gauge bosons W_R, Z_R and doubly charged Higgs bosons $H^{\pm\pm}_{L,R}$) is also determined by v_R, resulting in a rich phenomenology at the LHC if $v_R \sim$ TeV [6],[7].

The Yukawa coupling h_{ij} mediates many low energy LFV processes. In this paper we consider the impact of $H^{\pm\pm}_{L,R}$ on the branching ratio (BR) of the LFV decays $\tau \to l_i l_j l_k$ and $\mu \to e\gamma$ in the context of the LR symmetric model [8],[9]. Experimental prospects for $\mu \to e\gamma$ are bright with the imminent commencement of the MEG experiment which will probe BR$\sim 10^{-13} \to 10^{-14}$, two to three orders of magnitude beyond the current upper limit [10]. At the e^+e^- B factories limits of the order BR$(\tau \to l_i l_j l_k) < 10^{-7}$ with ~ 90 fb^{-1} [11],[12] have been obtained utilizing direct $e^+e^- \to \tau^+\tau^-$ production. Simulations of the detection prospects at a proposed high luminosity e^+e^- B factory with $\mathcal{L}$=5$\to$ 50 ab^{-1} anticipate sensitivity to BR$\sim 10^{-8} \to 10^{-9}$ [13]. Additional searches can be performed at the LHC where τ leptons are copiously produced from the decays of W, Z, B, D, with anticipated sensitivities to BR$\sim 10^{-8}$ [14].

In the LR symmetric model $H^{\pm\pm}_{L,R}$ mediate $\tau \to l_i l_j l_k$ at *tree-level* due to an effective 4-Fermi charged lepton interaction proportional to $h^*_{\tau i} h_{jk}/M^2_{H^{\pm\pm}}$. Hence such a model can comfortably accommodate BRs of order $10^{-7} \to 10^{-9}$ which will be probed at current and forthcoming experiments. For the loop induced decays $\mu \to e\gamma$ and $\tau \to l\gamma$ the dominant contribution in the LR symmetric model originates from diagrams involving $H^{\pm\pm}_{L,R}$. In the LR model one has BR$(\tau \to lll) \gg$ BR$(\tau \to l\gamma)$, which contrasts with the general expectation BR$(\tau \to$

$l\gamma) \gg$BR($\tau \to lll$) for models in which the tree-level $\tau \to l_i l_j l_k$ interaction is absent (for scenarios where BR($\tau \to l\gamma$) $\sim$BR($\tau \to lll$) is possible see [15]). Due to the larger backgrounds for the search for $\tau \to l\gamma$, the experimental sensitivity to BR($\tau \to l\gamma$) at the e^+e^- B factories is expected to be inferior to that for $\tau \to l_i l_j l_k$ [13]. Consequently the hierarchy BR($\tau \to lll$) $\gg$ BR($\tau \to l\gamma$) in the LR model affords more promising detection prospects.

The presence of the above tree-level 4-Fermi interaction would also mediate the decay $\mu \to eee$ for which there is a strict bound ($< 10^{-12}$ [16]) at least three orders of magnitude stronger than the anticipated experimental sensitivity to $\tau \to lll$. Hence obtaining BR($\tau \to lll$) $> 10^{-9}$ together with compliance of the above bound on BR($\mu \to eee$) restricts the structure of h_{ij}. In the LR model we consider a specific ansatz for h_{ij} motivated by the observed pattern of the neutrino mixing angles, and perform a numerical study of the magnitude of BR($\tau \to l_i l_j l_k$).

Observation of BR($\tau \to lll$) $> 10^{-9}$ would be a spectacular signal of LFV and could be readily accommodated by a tree-level 4-Fermi coupling such as $h^*_{\tau i} h_{jk}/M^2_{H^{\pm\pm}}$ in the LR model. However, other models which contain a $H_L^{\pm\pm}$ or $H_R^{\pm\pm}$ with an analogous h_{ij} leptonic Yukawa coupling can cause a similar enhancement of BR($\tau \to lll$). If a signal were established for $\tau \to lll$ the angular distribution of the leptons can act as powerful discriminator of the models [17]. Such studies could be carried out at a high luminosity e^+e^- B factory [13].

Our work is organized as follows. In section 2 the manifest LR symmetric model is briefly reviewed. In section 3 a numerical analysis of BR($\tau \to lll$) and BR($\mu \to e\gamma$) is presented. In section 4 we discuss how to discriminate the LR model from other models which contain a $H^{\pm\pm}$ by means of angular asymmetries in the LFV decays. Conclusions are contained in section 5.

2 Left-Right Symmetric Model

The Left-Right (LR) symmetric model is an extension of the Standard Model (SM) based on the gauge group $SU(2)_R \otimes SU(2)_L \otimes U(1)_{B-L}$. The LR symmetric model has many virtues, e.g. i) the restoration of parity as an original symmetry of the Lagrangian which is broken spontaneously by a Higgs vev, and ii) the replacement of the arbitrary SM hypercharge Y by the theoretically more attractive $B - L$. Although the Higgs sector is arbitrary, a theoretically and phenomenologically appealing way to break the $SU(2)_R$ gauge symmetry is by invoking Higgs isospin triplet representations. Such a choice conveniently allows the implementation of a low energy seesaw mechanism for neutrino masses. The vev of the neutral member of the right-handed triplet (v_R) can be chosen to give a TeV scale Majorana mass term for the right-handed neutrinos, while the bidoublet Higgs fields provide the small Dirac mass, leading to light masses for the observed neutrinos. The above LR symmetric model predicts several new particles, among which the new gauge bosons W_R, Z_R and doubly charged scalars $H_L^{\pm\pm}$, $H_R^{\pm\pm}$ [18] have impressive discovery potential at hadron colliders if $v_R = \mathcal{O}$ (1-10) TeV due to their large cross-sections and/or low background signatures.

Experiments which search for LFV decays of μ and τ provide a complementary way of probing the LR symmetric model. A comprehensive study of $\mu \to e\gamma$, $\mu \to eee$ and $\mu \to e$ conversion in the present model was performed in [9]. However, the recent termination of the MECO ($\mu \to e$ conversion) experiment together with no immediate improvement for the SINDRUM collaboration limit BR($\mu \to eee$) $< 10^{-12}$ [16] leaves $\mu \to e\gamma$ as the only means of

testing the LR model in LFV processes involving μ in the near future [10].

An alternative probe of the LR model which was not developed in [9] are the LFV decays $\tau \to l_i l_j l_k$. Although the experimental sensitivity is inferior to that for the above processes involving μ, the decays $\tau \to l_i l_j l_k$ have the virtue of probing many combinations of the triplet Higgs-lepton-lepton Yukawa h_{ij} couplings. We introduce various strutures for the arbitrary h_{ij} motivated by the currently preferred bi-large mixing form of the Maki-Nakagawa-Sakata [19] (MNS) matrix. Should a signal for $\tau \to lll$ and/or $\mu \to e\gamma$ be observed, the angular distribution of the final state leptons can provide a means of distinguishing models with $H^{\pm\pm}$. We now briefly introduce the LR model and present the relevant formulae for the numerical discussion in Section 3. For a detailed introduction we refer the reader to [20].

The quarks and leptons are assigned to multiplets with quantum numbers $(T_L, T_R, B-L)$:

$$\begin{aligned} Q_{iL} &= \begin{pmatrix} u_i' \\ d_i' \end{pmatrix}_L : (1/2:0:1/3)\,,\ Q_{iR} = \begin{pmatrix} u_i' \\ d_i' \end{pmatrix}_R : (0:1/2:1/3)\ , \\ L_{iL} &= \begin{pmatrix} \nu_i' \\ l_i' \end{pmatrix}_L : (1/2:0:-1)\,,\ L_{iR} = \begin{pmatrix} \nu_i' \\ l_i' \end{pmatrix}_R : (0:1/2:-1)\ . \end{aligned} \tag{1}$$

Here $i = 1,2,3$ denote generation number. The spontaneous symmetry breaking to $U(1)_{em}$ occurs through the Higgs mechanism. The Higgs sector consists of a bidoublet Higgs field, Φ, and two triplet Higgs fields, Δ_L and Δ_R:

$$\begin{aligned} \Phi = \begin{pmatrix} \phi_1^0 & \phi_2^+ \\ \phi_1^- & \phi_2^0 \end{pmatrix} \quad &: \quad (1/2:1/2:0)\ , \\ \Delta_L = \begin{pmatrix} \delta_L^+/\sqrt{2} & \delta_L^{++} \\ \delta_L^0 & -{\delta_L}^+/\sqrt{2} \end{pmatrix} : (1:0:2)\ , \Delta_R &= \begin{pmatrix} \delta_R^+/\sqrt{2} & \delta_R^{++} \\ \delta_R^0 & -{\delta_R}^+/\sqrt{2} \end{pmatrix} : (0:1:2)\ . \end{aligned} \tag{2}$$

The vevs for these fields are as follows:

$$\langle\Phi\rangle = \begin{pmatrix} \kappa_1/\sqrt{2} & 0 \\ 0 & \kappa_2/\sqrt{2} \end{pmatrix},\ \langle\Delta_L\rangle = \begin{pmatrix} 0 & 0 \\ v_L/\sqrt{2} & 0 \end{pmatrix}\ ,\ \langle\Delta_R\rangle = \begin{pmatrix} 0 & 0 \\ v_R/\sqrt{2} & 0 \end{pmatrix}\ . \tag{3}$$

The gauge groups $SU(2)_R$ and $U(1)_{B-L}$ are spontaneously broken at the scale v_R. Phenomenological considerations require $v_R \gg \kappa = \sqrt{\kappa_1^2 + \kappa_2^2} \sim \frac{2M_{W_1}}{g}$ (EW scale). The vev v_L does not play a role in the breaking of the gauge symmetries and is constrained to be small ($v_L < 8$ GeV) in order to comply with the measurement of $\rho = M_Z \cos\theta_W / M_W \sim 1$. The LR model predicts six neutral Higgs bosons, two singly charged Higgs bosons, and two doubly charged Higgs bosons. The Lagrangian is required to be the invariant under the discrete left-right symmetry: $Q_L \leftrightarrow Q_R$, $L_L \leftrightarrow L_R$, $\Delta_L \leftrightarrow \Delta_R$, $\Phi \leftrightarrow \Phi^\dagger$. This ensures equal gauge couplings ($g_L = g_R = g$) for $SU(2)_L$ and $SU(2)_R$.

The leptonic Yukawa interactions are as follows:

$$-\mathcal{L}^{yuk} = \bar{L}_L(y_D\Phi + \tilde{y}_D\tilde{\Phi})L_R + iy_M(L_L^T C\tau_2\Delta_L L_L + L_R^T C\tau_2\Delta_R L_R) + h.c.\ . \tag{4}$$

Here $\tilde{\Phi} \equiv \tau_2\Phi^*\tau_2$; $y_D, \tilde{y}_D$ are Dirac type Yukawa coupling; y_M is a 3×3 Majorana type Yukawa coupling matrix which will lead to Majorana neutrino masses (see below) and is the primary

motivation for introducing the Higgs triplet representations Δ_L and Δ_R. Invariance under the left-right discrete symmetry gives $y_D = y_D^\dagger$, $\tilde{y}_D = \tilde{y}_D^\dagger$ and $y_M = y_M^T$. The 3×3 mass matrix for charged leptons is:

$$M_l = \frac{1}{\sqrt{2}}(y_D \kappa_2 + \tilde{y}_D \kappa_1) \ , \tag{5}$$

which is diagonalized by the unitary matrices, V_L^l and V_R^l, as:

$$V_L^{l\dagger} M_l V_R^l = diag(m_e, m_\mu, m_\tau) \ . \tag{6}$$

The Lagrangian for the neutrino masses is:

$$-\mathcal{L}_{mass} = \frac{1}{2}(\bar{n}_L^c M_\nu n_R + \bar{n}_R M_\nu^* n_L^c) \, , \tag{7}$$

where $n_L^c = (\nu_L, \nu_R^c)^T$ and $n_R = (\nu_L^c, \nu_R)^T$ with the definition of $\nu_R^c = C(\bar{\nu_R})^T$. The 6×6 mass matrix for the neutrinos can be written in the block form:

$$M_\nu = \begin{pmatrix} M_L & m_D \\ m_D^T & M_R \end{pmatrix} . \tag{8}$$

Each entry is given by:

$$m_D = \frac{1}{\sqrt{2}} (y_D \kappa_1 + \tilde{y}_D \kappa_2) \ , \tag{9}$$

$$M_R = \sqrt{2} y_M v_R \ , \tag{10}$$

$$M_L = \sqrt{2} y_M v_L \ . \tag{11}$$

The neutrino mass matrix is diagonalized by a 6×6 unitary matrix V as $V^T M_\nu V = M_\nu^{diag} = diag(m_1, m_2, m_3, M_1, M_2, M_3)$, where m_i and M_i are the masses for neutrino mass eigenstates:

$$V \equiv \begin{pmatrix} V_L^{\nu *} & V_L^{\nu' *} \\ V_R^{\nu'} & V_R^{\nu} \end{pmatrix} \ . \tag{12}$$

The small neutrino masses m_i are generated by the Type II seesaw mechanism. Obtaining eV scale neutrino masses with $y_M = \mathcal{O}(0.1 - 1)$ requires M_L (and consequently v_L) to be eV scale. However, the minimization of the Higgs potential leads to a relationship among the vevs, $v_L \sim \gamma \kappa^2 / v_R$, where γ is a function (introduced in [7]) of scalar quartic couplings β_i and ρ_i. For natural values of β_i and ρ_i one has $\gamma \sim 1$ and thus v_L would be $\mathcal{O}(1 - 10)$ GeV for $v_R \sim$ TeV. Reducing v_L to the eV scale to order to comply with the observed neutrino mass scale would require severe fine-tuning $\gamma < 10^{-7}$. In LR model phenomenology it is conventional to set $\beta_i = 0$ (and hence $\gamma = 0$) which ensures $v_L = 0$. Henceforth we will take $v_L = 0$ for which the masses of the light neutrinos arise from from Type I seesaw mechanism and are approximately $m_i \sim m_D^2 / M_R$. [1] In order to realize the low energy ($\sim \mathcal{O}(1 - 10)$ TeV) scale

[1] For an alternative approach which maintains the Type II seesaw mechanism and obtains $v_L \sim$eV by means of horizontal symmetries see [21].

for the right-handed Majorana neutrinos, the Dirac mass term m_D should be $\mathcal{O}$ (MeV), which for $\kappa_2 \sim 0$ corresponds to $y_D \sim 10^{-6}$ (i.e. comparable in magnitude to the electron Yukawa coupling).

There are two physical singly charged Higgs bosons, $H_1^\pm$ and $H_2^\pm$, which are linear combinations of the singly charged scalar fields residing in Φ, Δ_L and Δ_R. The leptonic couplings $\tilde{y}_D$ of $H_2^\pm$ (which is essentially composed of $\phi_1^\pm$ and $\phi_2^\pm$) are of order m_l/m_W and can be neglected compared to leptonic Yukawa couplings for the triplet field $H_1^\pm \sim \delta_L^\pm$ which are unrelated to fermion masses and may be sizeable. The interaction of $H_1^\pm$ with leptons is as follows (where $P_{L,R} = (1 \mp \gamma_5)/2$):

$$\mathcal{L}_{H_1^\pm} = \sqrt{2}\Big[H_1^+ \, \overline{N}\left(\tilde{h}\, P_L\right) l + H_1^- \, \overline{l}\left(\tilde{h}^\dagger \, P_R\right) N\Big] \, . \tag{13}$$

The LFV interactions of leptons with doubly charged Higgs bosons (where $H_L^{\pm\pm} = \delta_L^{\pm\pm}, H_R^{\pm\pm} = \delta_R^{\pm\pm}$ for $v_L = 0$) are given by:

$$\mathcal{L}_{H_{L,R}^{\pm\pm}} = \Big[H_{L,R}^{++} \, \overline{l^c}\,(h_{L,R}\, P_{L,R})\, l + H_{L,R}^{--} \, \overline{l}\left(h_{L,R}^\dagger \, P_{R,L}\right) l^c\Big] \, . \tag{14}$$

The LFV coupling matrices in Eq.(13) and Eq.(14) are respectively given by:

$$\tilde{h} = \frac{1}{\sqrt{2}v_R} V_L^{\nu T} M_R V_L^l \, , \tag{15}$$

$$h_L = \frac{1}{\sqrt{2}v_R} V_L^{lT} M_R V_L^l \, , \tag{16}$$

$$h_R = \frac{1}{\sqrt{2}v_R} V_R^{lT} M_R V_R^l \, . \tag{17}$$

Here $V_R^{\nu T} M_R V_R^\nu \simeq M = diag(M_1, M_2, M_3)$. The mass matrix for the charged vector bosons is:

$$\tilde{M}_W^2 = \frac{g^2}{4} \begin{pmatrix} \kappa^2 & -2\kappa_1\kappa_2 \\ -2\kappa_1\kappa_2 & \kappa^2 + 2v_R^2 \end{pmatrix} \, . \tag{18}$$

This is diagonalized via the mixing angle $\xi = -\tan^{-1}\left(2\kappa_1\kappa_2/v_R^2\right)/2$ with the eigenvalues $M_{W_{1,2}}^2 = g^2\left(\kappa^2 + v_R^2 \mp \sqrt{v_R^4 + 4\kappa_1^2\kappa_2^2}\right)/4$:

$$W_L = \cos\xi \, W_1 + \sin\xi \, W_2, \qquad W_R = -\sin\xi \, W_1 + \cos\xi \, W_2 \, . \tag{19}$$

The strong experimental constraint on the mixing angle ($\xi < 10^{-3}$) [31] enforces one of κ_1, κ_2 to be small if $v_R = \mathcal{O}$ (TeV). Neglecting such small mixing between W_1 and W_2, the LFV interactions with the gauge bosons are as follows:

$$\begin{aligned} \mathcal{L}_{CC} = \frac{g}{\sqrt{2}}\Big\{ & \overline{N}\Big[\gamma^\mu \, P_R\,(K_R)\Big] l \cdot {W_2^+}_\mu + \overline{l}\Big[\gamma^\mu \, P_R\,(K_R^\dagger)\Big] N \cdot {W_2^-}_\mu \\ & + \overline{N}\Big[\gamma^\mu \, P_L\,(K_L)\Big] l \cdot {W_1^+}_\mu + \overline{l}\Big[\gamma^\mu \, P_L\,(K_L^\dagger)\Big] N \cdot {W_1^-}_\mu \Big\} \, , \end{aligned} \tag{20}$$

where K_L and K_R are the 6×3 LFV coupling matrices which are respectively written as:

$$K_L = \begin{pmatrix} V_L^{\nu\dagger} V_L^l \\ V_L^{\nu'\dagger} V_L^l \end{pmatrix} = \begin{pmatrix} V_{\rm MNS}^\dagger \\ V_L^{\nu'\dagger} V_L^l \end{pmatrix} , \quad K_R = \begin{pmatrix} V_R^{\nu'\dagger} V_R^l \\ V_R^{\nu\dagger} V_R^l \end{pmatrix} . \tag{21}$$

The upper 3×3 block in K_L can be identified as the hermitian conjugate of the MNS matrix $V_{\rm MNS}$.

2.1 Manifest LR Symmetric Model

In the LR model the mixing matrices for the left and right fermions are in general not equal e.g. for the lepton sector $V_L^l \neq V_R^l$. The special case of $V_L^l = V_R^l$ is referred to as the "Manifest LR symmetric model" and arises in either of the following scenarios: i) both κ_1 and κ_2 are real, or ii) one of κ_1 and κ_2 is identically zero. In our numerical analysis we will set $\kappa_2 = 0$, which has the virtue of eliminating $W_L - W_R$ mixing and in some cases (for specific forms of the Higgs potential) is required to suppress FCNCs and preserve unitarity in the LR model [6]. In the Manifest LR symmetric model one has the additional constraint $m_D = m_D^\dagger$ which must be respected when evaluating the magnitude of the LFV processes.

A further important consequence of the Manifest LR symmetric model is the relationship $h_L = h_R \equiv h$ which can be derived from Eq.(16) and Eq.(17). Using K_L and K_R in Eq.(21), the LFV couplings for the interactions of leptons with singly and doubly charged Higgs bosons are as follows:

$$\tilde{h} = K_L^* h \ , \qquad h = \frac{1}{\sqrt{2} v_R} K_R^T \, M_\nu^{\rm diag} \, K_R \ . \tag{22}$$

At leading order in m_D/M_R, one may express h by:

$$h_{ij} = \sum_{n={\rm heavy}} \Big(K_R\Big)_{ni} \Big(K_R\Big)_{nj} \sqrt{x_n} \ , \tag{23}$$

$$x_n = \left(\frac{M_n}{\sqrt{2} v_R}\right)^2 \ . \tag{24}$$

2.2 Effective Lagrangian and branching ratios for the LFV processes

2.2.1 4-lepton interactions

The effective Lagrangian for 4-lepton interactions is as follows:

$$\mathcal{L} = \frac{1}{2} (h^*)_{mi} (h)_{jk} \left\{ \frac{1}{M_{H_L^{\pm\pm}}^2} \Big(\bar{l}_m \gamma^\mu P_L l_k\Big) \Big(\bar{l}_i \gamma_\mu P_L l_j\Big) + \frac{1}{M_{H_R^{\pm\pm}}^2} \Big(\bar{l}_m \gamma^\mu P_R l_k\Big) \Big(\bar{l}_i \gamma_\mu P_R l_j\Big) \right\} \ . \tag{25}$$

The branching ratio for $\tau \to l_i l_j l_k$ is given by:

$$BR(\tau \to l_i l_j l_k) = \frac{8S}{g^4} |h_{\tau l_i}^* h_{l_j l_k}|^2 \left(\frac{M_{W_1}^4}{M_{H_L^{\pm\pm}}^4} + \frac{M_{W_1}^4}{M_{H_R^{\pm\pm}}^4} \right) BR(\tau \to \mu\nu\nu) \ . \tag{26}$$

Here S=1 (2) for $j = k$ ($j \neq k$). In the LR model one may express h_{ij} in terms of $K_R K_R$ via Eq.(23). However, the above form Eq.(26) can be applied to other models with $H_L^{\pm\pm}$ and $H_R^{\pm\pm}$ for which no identity Eq.(23) exists.

2.2.2 $\mu \to e\gamma$

The effective Lagrangian for $\mu \to e\gamma$ is as follows:

$$\mathcal{L} = -\frac{4G}{\sqrt{2}} \left\{ m_\mu A_R \overline{\mu} \sigma^{\mu\nu} P_L e F_{\mu\nu} + m_\mu A_L \overline{\mu} \sigma^{\mu\nu} P_R e F_{\mu\nu} + h.c. \right\} \ . \tag{27}$$

A_L receives contributions from $W_2 - N_i$ and $H_R^{\pm\pm}$ and is given by [9]:

$$A_L \ = \ \frac{1}{16\pi^2} \sum_{n=\text{heavy}} \left(K_R^\dagger\right)_{en} \left(K_R\right)_{n\mu} \ \left[\frac{M_{W_1}^2}{M_{W_2}^2} S_3(x_n) - \frac{x_n}{3} \frac{M_{W_1}^2}{M_{H_R^{\pm\pm}}^2} \right] \ , \tag{28}$$

where

$$S_3(x_n) = -\frac{x(1+2x)}{8(1-x^2)^2} + \frac{3x^2}{4(1-x)^2} \left\{ \frac{x}{(1-x)^2}(1 - x + \log x) + 1 \right\} \ . \tag{29}$$

A_R receives contributions from $H_L^{\pm\pm}$ and $H_1^\pm$ and is given explicitly by [9]:

$$A_R \ = \ \frac{1}{16\pi^2} \sum_{n=\text{heavy}} \left(K_R^\dagger\right)_{en} \left(K_R\right)_{n\mu} \ x_n \left[-\frac{1}{3} \frac{M_{W_1}^2}{M_{H_L^{\pm\pm}}^2} - \frac{1}{24} \frac{M_{W_1}^2}{M_{H_1^\pm}^2} \right] \ . \tag{30}$$

The branching ratio for $\mu \to e\gamma$ is given by: [2]

$$BR(\mu \to e\gamma) = 384\pi^2 e^2 (|A_L|^2 + |A_R|^2). \tag{31}$$

3 Numerical analysis for BR($\tau \to lll$) and BR($\mu \to e\gamma$)

The LFV decays $\tau \to lll$ are the analogy of $\mu \to eee$ and provide sensitive probes of the h_{ij} couplings in the LR model. Mere observation of such a decay would constitute a spectacular signal of physics beyond the SM. There are six distinct decays for $\tau^+ \to lll$ (likewise for τ^-): $\tau^+ \to \mu^+\mu^+\mu^-$, $\tau^+ \to e^+e^+e^-$, $\tau^+ \to \mu^+\mu^+e^-$, $\tau^+ \to \mu^+\mu^-e^+$, $\tau^+ \to e^+e^+\mu^-$, $\tau^+ \to e^+e^-\mu^+$. Searches for all six decays have been performed by BABAR (91 fb^{-1}) [12] and BELLE (87 fb^{-1}) [11]. Upper limits of the order BR($\tau \to lll$) $< 2 \times 10^{-7}$ were derived. Although these limits are several orders of magnitude weaker than the bound BR($\mu \to eee$) $< 10^{-12}$, they have the virtue of constraining many combinations of the h_{ij} couplings in the context of the LR model. Moreover, greater sensitivity to BR($\tau \to lll$) is expected from forthcoming experiments. A proposed Super B Factory anticipates sensitivity to BR($\tau \to lll$) $\sim 10^{-8}$ and 10^{-9} for 5 ab^{-1} and 50 ab^{-1} respectively [13]. At the LHC, τ can be copiously produced from several sources (from B/D decay and direct production via $pp \to W \to \tau\nu$, $pp \to Z \to \tau^+\tau^-$) and sensitivity to BR($\tau \to lll$) $> 10^{-8}$ is claimed [14]. Such low BRs can be reached due to the very small SM background. In contrast, the background to $\tau \to l\gamma$ is non-negligible and might prevent the B factories from probing below BR$\sim 10^{-8}$. In addition, one expects BR($\tau \to lll$) $\gg$ BR($\tau \to l\gamma$) in the LR symmetric model and thus the former decay is the more effective probe. We note

[2] In our numerical analysis we do not include a suppression factor of $\sim 15\%$ arising from electromagnetic corrections [32].

that other rare LFV τ decays involving quark final states will not arise in the LR model since h_{ij} mediates processes involving leptons only. Hence we shall only focus on $\tau \to lll$. In our numerical analysis only the stringent constraint from $\mu \to eee$ is imposed. Other constraints on h_{ij} (e.g. the anomalous magnetic moment of μ $(g-2)$, Bhabha scattering and other LFV processes - see [22]) are considerably weaker and are neglected.

The magnitude of h_{ij} cannot be predicted from the neutrino oscillation data alone since it is related to the physics at $\mathrm{SU}(2)_R$ breaking scale. However, h_{ij} also crucially depends on the mixing matrix in the charged lepton sector V_L^l:

$$h = \frac{1}{\sqrt{2}v_R} V_L^{lT} M_R V_L^l \ , \tag{32}$$

where M_R is non-diagonal in general. Since V_L also enters the MNS matrix:

$$V_{\mathrm{MNS}} = V_L^{l\dagger} V_L^{\nu} \ , \tag{33}$$

we will introduce 4 distinct structures for V_L^l motivated by the bi-large mixing form of V_{MNS} and perform a quantitative analysis of the magnitude of h_{ij} (and consequently $\mathrm{BR}(\tau \to lll)$) in the LR model.

In order to establish our formalism we first explicitly present the standard parametrisation of the MNS matrix:

$$\begin{aligned} V_{\mathrm{MNS}} &= \begin{pmatrix} 1 & 0 & 0 \\ 0 & c_{23} & s_{23} \\ 0 & -s_{23} & c_{23} \end{pmatrix} \begin{pmatrix} c_{13} & 0 & s_{13}e^{-i\delta} \\ 0 & 1 & 0 \\ -s_{13}e^{i\delta} & 0 & c_{13} \end{pmatrix} \begin{pmatrix} c_{12} & s_{12} & 0 \\ -s_{12} & c_{12} & 0 \\ 0 & 0 & 1 \end{pmatrix} \\ &= U(\theta_{23})U(\theta_{13})U(\theta_{12}) \ . \end{aligned} \tag{34}$$

Here s_{ij} (c_{ij}) represents $\sin\theta_{ij}$ ($\cos\theta_{ij}$) and the unitary matrices $U(\theta_{23})$, $U(\theta_{13})$, and $U(\theta_{12})$ are responsible for mixing between 2-3, 1-3, and 1-2 elements respectively.

The angles θ_{12} and θ_{23} are measured with relatively good accuracy in the solar and atmospheric neutrino oscillation experiments respectively. The solar and KamLAND reactor neutrino oscillation experiments [23],[24] provide the following constraints on the mixing angle θ_{12} and the mass-squared difference of $\Delta m_{12}^2 = m_2^2 - m_1^2$: $\sin^2\theta_{12} \sim 0.31$, $\Delta m_{12}^2 \sim 8 \times 10^{-5}\ \mathrm{eV}^2$. The mixing angle θ_{23} and the mass-squared difference Δm_{13}^2 measured in the atmospheric neutrino oscillation are as follows [25],[26]: $\sin^2 2\theta_{23} \sim 1.0$, $|\Delta m_{13}^2| \sim 2.6 \times 10^{-3}\ \mathrm{eV}^2$. An upper bound on the remaining angle θ_{13} has been obtained from the CHOOZ and Palo Verde reactor neutrino oscillation experiments [27],[28]: $\sin\theta_{13} \lesssim 0.2$.

The ignorance of the sign of Δm_{13}^2 and the absolute neutrino mass scale leads to the following three neutrino mass patterns which are consistent with current oscillation data: Normal hierarchy (NH) $m_1 < m_2 \ll m_3$; Inverted hierarchy (IH) $m_3 \ll m_1 < m_2$; Quasi degeneracy (DG) $m_1 \sim m_2 \sim m_3$. Data from WMAP [29] provides the following constraint on the sum of the light neutrino masses: $\sum_{i=1,2,3} m_i < 2$ eV. However, LFV processes in the LR model do not depend sensitively on the neutrino mass pattern.

In order to perform our numerical analysis of the magnitude of $\mathrm{BR}(\tau \to lll)$ and $\mathrm{BR}(\mu \to e\gamma)$ we introduce the following four specific cases:

CASE	$V_L^{l\dagger}$	V_L^{ν}
I	$-iV_{\rm MNS}$	iI
II	$-iU(\theta_{23})U(\theta_{13})$	$iU(\theta_{12})$
III	$-iU(\theta_{23})$	$iU(\theta_{13})U(\theta_{12})$
IV	$-iI$	$iV_{\rm MNS}$

Here I represents a unit matrix. In CASE I (IV) both large mixings in $V_{\rm MNS}$ originate from the charged lepton (neutrino) mixing matrix. Each case has distinct ways of satisfying the stringent bound BR($\mu \to eee$) $< 10^{-12}$. In our numerical analysis we will assume multi-TeV scale masses for $H_L^{\pm\pm}$ and $H_R^{\pm\pm}$ which renders direct detection improbable at the LHC. For $M_{H_L^{\pm\pm}}$,$M_{H_R^{\pm\pm}} < 1$ TeV the LHC has excellent discovery prospects in the channels $H^{\pm\pm} \to l_i^{\pm} l_j^{\pm}$ [18] (especially for $l_{i,j} = e, \mu$). Observation of $H_{L,R}^{\pm\pm}$ (which would provide a measurement of $M_{H^{\pm\pm}}$) together with a signal for $\tau \to l_i l_j l_k$ would permit a measurement of the coupling combination $|h^*_{\tau i} h_{jk}|$.

We wish to study the magnitude of BR($\tau \to lll$) and BR($\mu \to e\gamma$) in the parameter space with a phenomenologically acceptable neutrino mass matrix. In the LR model the light neutrino masses arise from the seesaw mechanism and are approximately as follows:

$$m_\nu = -m_D M_R^{-1} m_D^T \ . \tag{35}$$

At the leading order, m_ν is diagonalized by V_L^ν:

$$m_\nu \ \simeq \ V_L^\nu m_\nu^{diag} V_L^{\nu T} \ , \tag{36}$$

where $m_\nu^{diag} = diag(m_1, m_2, m_3)$. The Dirac mass matrix m_D depends on an arbitrary Yukawa coupling y_D. As advocated in [30], it is beneficial to parametrize a general seesaw type matrix such that the arbitrary m_D is replaced by potential observables i.e. the heavy and light neutrino masses. We will apply the formalism of [30] in our numerical analysis, with the additional constraint that the manifest LR model requires the Dirac mass matrix for both the neutrinos and charged leptons to be a hermitian matrix:

$$m_D = m_D^\dagger \ . \tag{37}$$

We introduce a complex orthogonal matrix R which satisfies $R^T R = 1$ and parametrize the neutrino Dirac mass matrix m_D as follows:

$$m_D = -iV_L^\nu \sqrt{m_\nu^{diag}} R^T \sqrt{M_R} \ . \tag{38}$$

The LFV processes are evaluated in the parameter space where there exists an R matrix which satisfies the condition Eq.(37). This condition guarantees a phenomenologically acceptable neutrino mass matrix and perturbative Yukawa coupling y_D. In our calculation, the Majorana phases in the MNS matrix are neglected while the CP conserving cases for the Dirac phase ($\delta = 0$ or π) are taken into account for simplicity. Without loss of generality we work in a basis where the right-handed neutrino mass matrix M_R is a real diagonal matrix, $M_R = diag(M_1, M_2, M_3)$, with $0 < M_1 \leq M_2 \leq M_3$. Neglecting CP violation, the condition Eq.(37) requires that V_L^ν is purely imaginary, while R is a real matrix. We stress that the LFV processes do not depend on the actual structure of R. However, proving the existence of an R matrix for each of the four cases (I, II, III, IV) ensures the validity of our numerical analysis.

3.1 Numerical results: CASE I

The bi-large mixing originates from the charged-lepton sector. Parametrizing the R matrix as:

$$R = U(\theta_{23}^R)U(\theta_{13}^R)U(\theta_{12}^R) \ , \tag{39}$$

the explicit form in CASE I is given as follows:

$$\theta_{12}^R = \theta_{23}^R = \theta_{13}^R = 0 \ . \tag{40}$$

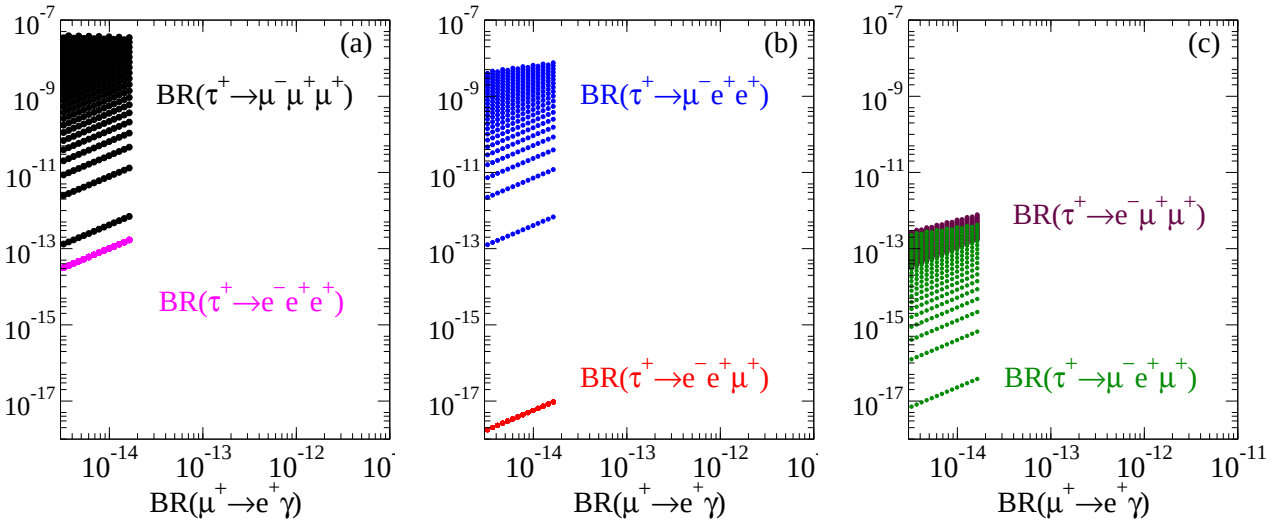

Figure 1: Branching ratios for (a) $\tau^+ \to e^-e^+e^+$ and $\tau^+ \to \mu^-\mu^+\mu^+$, (b) $\tau^+ \to e^-e^+\mu^+$ and $\tau^+ \to \mu^-e^+e^+$, and (c) $\tau^+ \to e^-\mu^+\mu^+$ and $\tau^+ \to \mu^-e^+\mu^+$ against BR($\mu^+ \to e^+\gamma$) for $s_{13} = 0$ in CASE I. The experimental bound on BR($\mu \to eee$) ($< 10^{-12}$) is imposed.

Using Eq.(32) the elements of h_{ij} in CASE I are as follows:

$$\sqrt{2}v_R h_{e\mu} = c_{12}s_{12}c_{23}c_{13}(M_2 - M_1) \pm c_{13}s_{13}s_{23}(M_3 - s_{12}^2 M_2 - c_{12}^2 M_1) \, , \tag{41}$$

$$\sqrt{2}v_R h_{e\tau} = -c_{12}s_{12}s_{23}c_{13}(M_2 - M_1) \pm c_{23}c_{13}s_{13}(M_3 - s_{12}^2 M_2 - c_{12}^2 M_1) \, , \tag{42}$$

$$\begin{aligned}\sqrt{2}v_R h_{\mu\tau} = {} & c_{23}s_{23}(c_{13}^2 M_3 - c_{12}^2 M_2 - s_{12}^2 M_1) \pm c_{12}s_{12}s_{13}((s_{23}^2 - c_{23}^2)M_2 + M_1) \\ & + c_{23}s_{23}s_{13}^2(s_{12}^2 M_2 - c_{12}^2 M_1) \, ,\end{aligned} \tag{43}$$

$$\sqrt{2}v_R h_{ee} = c_{13}^2(c_{12}^2 M_1 + s_{12}^2 M_2) + s_{13}^2 M_3 \, , \tag{44}$$

$$\begin{aligned}\sqrt{2}v_R h_{\mu\mu} = {} & c_{23}^2(s_{12}^2 M_1 + c_{12}^2 M_2) + s_{23}^2 c_{13}^2 M_3 \mp 2c_{12}s_{12}c_{23}s_{23}s_{13}(M_2 - M_1) \\ & + s_{23}^2 s_{13}^2(c_{12}^2 M_1 + s_{12}^2 M_2) \, .\end{aligned} \tag{45}$$

Here the upper (lower) sign is for Dirac phase $\delta = 0$ (π). It is clear that the off-diagonal elements in the h couplings vanish when all the heavy neutrinos are degenerate in mass, i.e. $M_1 = M_2 = M_3$. The strict bound on BR($\mu \to eee$) requires $|h_{e\mu}| \ll 1$ which leads to the following conditions:

$$\text{(i)} \quad M_1 \simeq M_2, \qquad s_{13}(M_3 - M_2) \simeq 0 \ , \tag{46}$$

$$\text{(ii)} \quad s_{13}M_3 \simeq c_{12}s_{12}(M_2 - M_1) + s_{13}(s_{12}^2 M_2 + c_{12}^2 M_1), \qquad \delta = \pi \ . \tag{47}$$

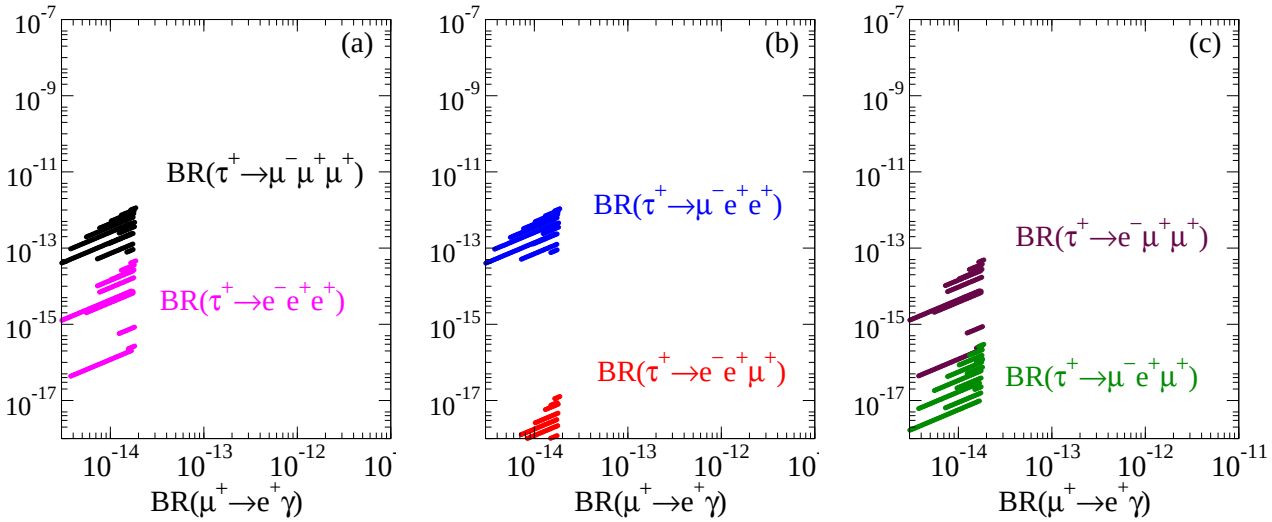

Figure 2: Branching ratios for (a) $\tau^+ \to e^-e^+e^+$ and $\tau^+ \to \mu^-\mu^+\mu^+$, (b) $\tau^+ \to e^-e^+\mu^+$ and $\tau^+ \to \mu^-e^+e^+$, and (c) $\tau^+ \to e^-\mu^+\mu^+$ and $\tau^+ \to \mu^-e^+\mu^+$ against $\mathrm{BR}(\mu^+ \to e^+\gamma)$ for $\sin\theta_{13} = 0.2$ with $\delta = 0$ in CASE I.

In (i) both terms contributing to $h_{e\mu}$ are zero, while in (ii) there a cancellation which ensures $|h_{e\mu}| \ll 1$.

We show the branching ratios for all six $\tau^+ \to lll$ decays against $\mathrm{BR}(\mu^+ \to e^+\gamma)$ for $s_{13} = 0$ in Fig.1. For simplicity we assume degeneracy for the masses of the heavy particles: $M_{W_2} = M_{H_L^{\pm\pm}} = M_{H_R^{\pm\pm}} = M_{H_1^{\pm}} = 3$ TeV. In our numerical analysis we vary the heavy neutrino masses randomly in the range 1 TeV $\leq M_i \leq 5$ TeV, with distributions that are flat on a logarithmic scale. This range is consistent with the vacuum stability condition for v_R given in [33].

In Fig.1 (a) ((b), (c)) the light and the dark points respectively denote the branching ratios for $\tau^+ \to e^-e^+e^+$ and $\tau^+ \to \mu^-\mu^+\mu^+$ ($\tau^+ \to e^-e^+\mu^+$ and $\tau^+ \to \mu^-e^+e^+$, $\tau^+ \to \mu^-e^+\mu^+$ and $\tau^+ \to e^-\mu^+\mu^+$). We impose the experimental constraint $\mathrm{BR}(\mu \to eee) < 10^{-12}$ which prevents a large mass difference between M_1 and M_2 when $s_{13} = 0$, as shown in condition (i) of Eq.(46). Among the six $\tau^+ \to lll$ decay modes the branching ratios of $\tau^+ \to \mu^-\mu^+\mu^+$ and $\tau^+ \to \mu^-e^+e^+$ can reach the anticipated sensitivity ($> 5 \times 10^{-9}$) of a future B factory. Such branching ratios are realized when the mass splitting $M_3 - M_2$ assumes larger values because $h_{\mu\tau}$ increases with it. On the other hand, the $\tau \to e$ transition is suppressed because $|h_{e\mu}| = |h_{e\tau}|$ for $s_{13} = 0$, and $|h_{e\mu}|$ is necessarily small in order to comply with the severe constraint from $\mu \to eee$. This can be seen for the light points in Fig.1 (a) where $\mathrm{BR}(\tau \to eee)$ is proportional to $\mathrm{BR}(\mu \to eee)$. Moreover, there is a strong correlation $\mathrm{BR}(\tau \to eee) \sim 10 \times \mathrm{BR}(\mu \to e\gamma)$. $\mathrm{BR}(\mu \to e\gamma)$ can be large as 10^{-14}, which is within the sensitivity of MEG experiment.

Figs.2 and 3 show the branching ratios for $\tau \to lll$ for $s_{13} = 0.2$ with the Dirac phase $\delta = 0$ and π respectively, imposing the constraint $\mathrm{BR}(\mu \to eee) < 10^{-12}$. For the other parameters we take the same values as in Fig.1. When $\delta = 0$ (Fig.2) all LFV processes are predicted to be small because of the small mass differences between the heavy neutrinos as shown in the condition (i). However, there is still the possibility of observing $\mu \to e\gamma$ at MEG experiment.

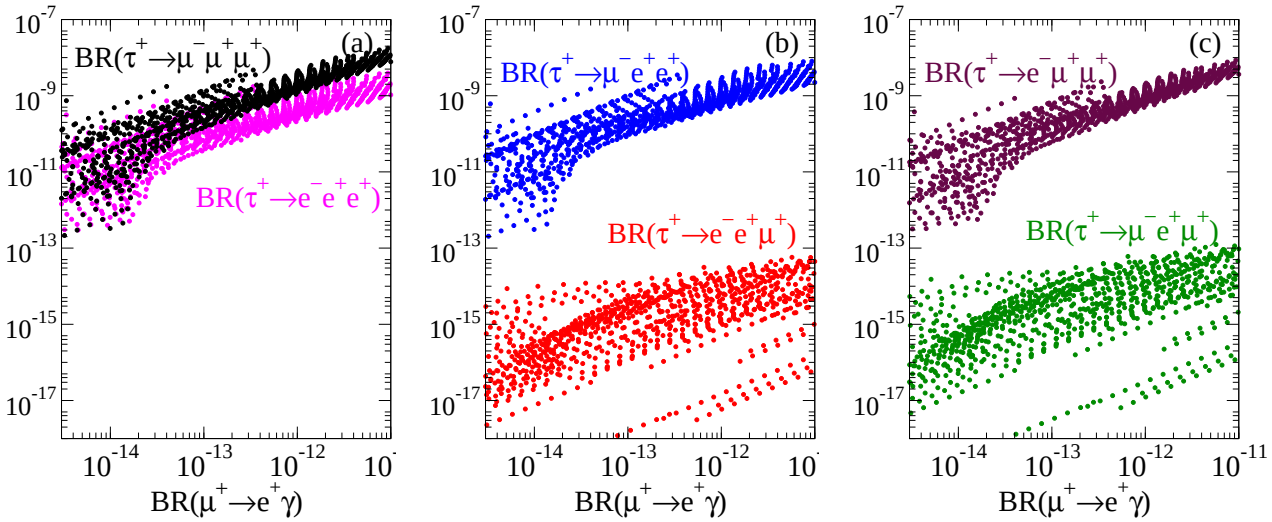

Figure 3: Branching ratios for (a) $\tau^+ \to e^-e^+e^+$ and $\tau^+ \to \mu^-\mu^+\mu^+$, (b) $\tau^+ \to e^-e^+\mu^+$ and $\tau^+ \to \mu^-e^+e^+$, and (c) $\tau^+ \to e^-\mu^+\mu^+$ and $\tau^+ \to \mu^-e^+\mu^+$ against $\mathrm{BR}(\mu^+ \to e^+\gamma)$ for $\sin\theta_{13} = 0.2$ with $\delta = \pi$ in CASE I.

On the other hand, taking $\delta = \pi$ (Fig.3) results in observable branching ratios for $\tau \to lll$. In this scenario one has $|h_{e\mu}| < |h_{e\tau}|$. Therefore the equality of $|h_{e\mu}|$ and $|h_{e\tau}|$ in Fig.1 is broken, which enables enhancement of $\mathrm{BR}(\tau^+ \to e^-e^+e^+)$ and $\mathrm{BR}(\tau^+ \to e^-\mu^+\mu^+)$ with simultaneous suppression of the $\mu \to e$ transition. Moreover, $\mathrm{BR}(\mu \to e\gamma)$ can be large, resulting in multiple signals of LFV processes.

3.2 Numerical results: CASE II

In this case the large mixing for the atmospheric angle originates from the charged lepton sector, while the large solar angle originates from the neutrino sector. The R matrix which satisfies the condition $m_D = m_D^\dagger$ is:

$$\tan\theta_{12}^R = \frac{\sqrt{M_1 m_1} + \sqrt{M_2 m_2}}{\sqrt{M_1 m_2} + \sqrt{M_2 m_1}} \tan\theta_{12} \ , \tag{48}$$

$$\theta_{23}^R = \theta_{13}^R = 0 \ . \tag{49}$$

The explicit form for h_{ij} is obtained from Eq.(41) - (45) by taking $s_{12} = 0$. The condition for suppressing $|h_{e\mu}|$ is:

$$s_{13}(M_3 - c_{12}^2 M_1) \simeq 0 \ , \tag{50}$$

which requires $s_{13} \simeq 0$ or $M_1 \simeq M_2 \simeq M_3$. In the latter case none of the $\tau \to lll$ decays are measurable, as in CASE I with $s_{13} = 0.2$ and $\delta = 0$. On the other hand, $h_{e\mu}$ and $h_{e\tau}$ are zero when $s_{13} = 0$, which results in vanishing branching ratios for $\tau^+ \to e^-l^+l^+, \mu^-e^+\mu^+$ and $\mu \to e\gamma$. Fig.4 shows the branching ratios for $\tau^+ \to \mu^-\mu^+\mu^+$ and $\tau^+ \to \mu^-e^+e^+$ against the heaviest neutrino mass M_3. Clearly the branching ratios increase with M_3 and for $M_3 > 3$ TeV observable rates are attained.

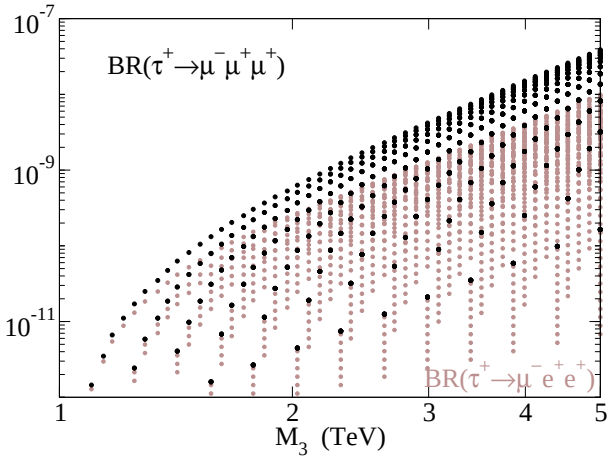

Figure 4: Branching ratios for $\tau^+ \to \mu^-\mu^+\mu^+$ and $\tau^+ \to \mu^- e^+ e^+$ against M_3 for $\sin\theta_{13} = 0$ in CASE II.

When $s_{13} \neq 0$ the magnitudes of each entry in h_{ij} are the same for $\delta = 0$ and π. We show in Fig.5 the branching ratios for $\tau \to lll$ decay against $\mathrm{BR}(\mu \to e\gamma)$ for $s_{13} = 0.2$. In order to satisfy the condition in Eq.(50) there cannot be large splittings among the masses of the heavy neutrinos. In this scenario only $\mathrm{BR}(\mu \to e\gamma)$ reaches the future experimental sensitivity.

3.3 Numerical Results: CASE III

In CASE III the constraint from $\mu \to eee$ is satisfied automatically since $h_{e\mu} = 0$ (obtained by setting $s_{12} = s_{13} = 0$ in Eq.(41). We obtain R as follows by treating θ_{13} as a perturbation:

$$\tan\theta_{12}^R = \frac{\sqrt{M_1 m_1} + \sqrt{M_2 m_2}}{\sqrt{M_1 m_2} + \sqrt{M_3 m_1}} \tan\theta_{12} \ , \tag{51}$$

$$\sin\theta_{23}^R = \frac{g}{f} s_{13} \ , \tag{52}$$

$$\begin{aligned} f =& M_3\sqrt{m_1 m_2} + \sqrt{M_3 m_3}\left\{\left(\sqrt{M_1 m_1} + \sqrt{M_2 m_2}\right) s_{12} s_{12}^R + \left(\sqrt{M_1 m_2} + \sqrt{M_2 m_1}\right) c_{12} c_{12}^R\right\} \\ &+ \sqrt{M_1 M_2} m_3 \ , \end{aligned} \tag{53}$$

$$\begin{aligned} g =& \sqrt{M_3} c_{12} s_{12}\left\{\left(\sqrt{M_2 m_1 m_2} + \sqrt{M_1} m_1\right) c_{12}^{R2} - \left(\sqrt{M_2 m_1 m_2} + \sqrt{M_1} m_2\right) s_{12}^{R2}\right\} \\ &+ \left\{\sqrt{M_2 M_3}(m_2 s_{12}^2 - m_1 c_{12}^2) + \sqrt{M_1 M_3 m_1 m_2}(s_{12}^2 - c_{12}^2)\right\} c_{12}^R s_{12}^R \\ &+ \sqrt{m_3}\left\{\left(\sqrt{M_1 M_2 m_2} + M_3\sqrt{m_1}\right) s_{12} c_{12}^R - \left(\sqrt{M_1 M_2 m_1} + M_3\sqrt{m_2}\right) c_{12} s_{12}^R\right\} \ , \end{aligned} \tag{54}$$

$$\sin\theta_{13}^R = \frac{\sqrt{M_3}(\sqrt{m_1} c_{12} s_{12}^R - \sqrt{m_2} s_{12} c_{12}^R) s_{23}^R + \left\{\sqrt{M_3 m_3} + \sqrt{M_1}(\sqrt{m_1} c_{12} c_{12}^R + \sqrt{m_2} s_{12} s_{12}^R)\right\} s_{13}}{\sqrt{M_1 m_3} + \sqrt{M_3}(\sqrt{m_1} c_{12} c_{12}^R + \sqrt{m_2} s_{12} s_{12}^R)} \ . \tag{55}$$

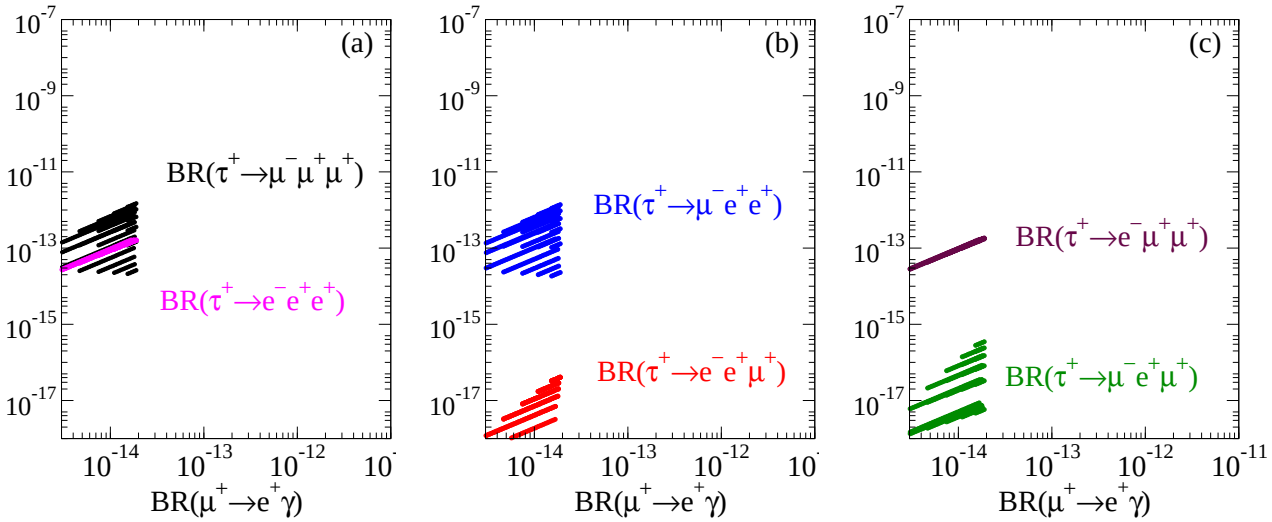

Figure 5: Branching ratios for (a) $\tau^+ \to e^-e^+e^+$ and $\tau^+ \to \mu^-\mu^+\mu^+$, (b) $\tau^+ \to e^-e^+\mu^+$ and $\tau^+ \to \mu^-e^+e^+$, and (c) $\tau^+ \to e^-\mu^+\mu^+$ and $\tau^+ \to \mu^-e^+\mu^+$ against BR($\mu \to e\gamma$) for $s_{13} = 0.2$ with $\delta = 0, \pi$ in CASE II.

CASE III predicts the same results as CASE II for the branching ratios of the LFV processes with $s_{13} = 0$ (Fig.4).

3.4 Numerical results: CASE IV

In this case the bi-large mixing originates from the neutrino sector. We checked the existence of R numerically. It is clear that none of the LFV processes are observed since h_{ij} is a diagonal matrix.

3.5 Summary

The numerical results of CASES I, II, III and IV for $M_{W_2} = M_{H_L^{\pm\pm}} = M_{H_R^{\pm\pm}} = M_{H_1^{\pm}} = 3$ TeV are qualitatively summarized in Table 1. It is clear that the number of observable rates for the LFV decays $\tau \to lll$ and $\mu \to e\gamma$ depends sensitively on the origin of the bi-large mixing in $V_{\rm MNS}$, with up to five signals being possible in the optimum scenario (CASE I with $\sin\theta_{13} = 0.2$, $\delta = \pi$). Hence future searches for $\tau \to lll$ and $\mu \to e\gamma$ provide insight into the structure of h_{ij} in the LR model.

Both BR($\tau \to lll$) and BR($\mu \to eee$) are inversely proportional to the fourth power of $M_{H^{\pm\pm}}$ (when $M_{H^{\pm\pm}} = M_{H_L^{\pm\pm}} = M_{H_R^{\pm\pm}}$) as shown in Eq.(26). Reducing M_{W_2}, $M_{H_L^{\pm\pm}}$, and $M_{H_R^{\pm\pm}}$ in all the figures would cause enhancement of BR($\tau \to lll$) and BR($\mu \to eee$) while maintaining the correlation. However, BR($\mu \to eee$) vanishes in CASE II with $s_{13} = 0$ and CASE III, and hence the strong bound BR($\mu \to eee$) $< 10^{-12}$ is automatically satisfied for any $M_{H^{\pm\pm}}$. In these latter cases the current experimental limits for BR($\tau \to lll$) can be reached and thus an upper bound on the heaviest neutrino mass M_3 can be derived (*e.g.* Fig.4 with $M_{W_2} = M_{H^{\pm\pm}} = 1.5$ TeV gives BR($\tau \to \mu\mu\mu$) $> 10^{-7}$ for $M_3 > 1.8$ TeV).

Table 1: LFV processes within the sensitivity of forthcoming or planned experiments for CASES I, II, III and IV with $M_{W_2} = M_{H_L^{\pm\pm}} = M_{H_R^{\pm\pm}} = M_{H_1^{\pm}} = 3$ TeV. BR$(\mu \to e\gamma) > 10^{-14}$ and BR$(\tau \to lll) > 10^{-9}$ is denoted by "$\surd$".

CASE	$\sin\theta_{13}$	δ	$\mu^+ \to e^+\gamma$	$\tau^+ \to e^-e^+e^+$	$\tau^+ \to e^-\mu^+\mu^+$	$\tau^+ \to \mu^-e^+e^+$	$\tau^+ \to \mu^-\mu^+\mu^+$
I	0		$\surd$			$\surd$	$\surd$
	0.2,	0	$\surd$				
	0.2,	π	$\surd$	$\surd$	$\surd$	$\surd$	$\surd$
II	0					$\surd$	$\surd$
	0.2,	0	$\surd$				
	0.2,	π	$\surd$				
III	0					$\surd$	$\surd$
	0.2,	0				$\surd$	$\surd$
	0.2,	π				$\surd$	$\surd$
IV	0						
	0.2,	0					
	0.2,	π					

We note here that the presented numerical results are for the scenario of all phases in $V_{\rm MNS}$ taken to be zero. We now briefly discuss the effect of including a non-zero Dirac phase ($\delta \neq 0$) in our analysis. In CASE I and CASE II the presence of $\delta \neq 0$ would not affect Eq.(38) since $U(\theta_{13})$ in Eq.(34) (which contains δ) only appears in V_L^l and not in V_L^ν. Thus the solution for the R matrix in the CP conserving case ($\delta = 0$ or π) also holds for the case of $\delta \neq 0$. Since V_L^l (which determines the LFV rates) has some dependence on δ we would expect minor changes in our numerical results but the same qualitative conclusions. In CASE III and IV the presence of $\delta \neq 0$ increases the number of free parameters in V_L^ν and no general solution for the R matrix can be found. However we expect that Eq.(37) will be satisfied in specific regions in the parameter space of M_i, and for CASE III some observable LFV rates might still be possible.

4 P odd Asymmetry for $\tau \to l_i l_j l_k$ and $\mu \to e\gamma$

From the preceding sections it is evident that both BR$(\tau \to lll)$ and BR$(\mu \to e\gamma)$ can be enhanced to experimental observability in the LR symmetric model. In particular, BR$(\tau \to lll) > 10^{-8}$ would be a signal suggestive of models which can mediate the decay at tree-level e.g. the LR model via virtual exchange of $H_{L,R}^{\pm\pm}$ [3] . If a signal were established for any of the six decays $\tau \to lll$, further information on the underlying model can be obtained by studying the angular distribution of the leptons. In this section we show that asymmetries can be defined which may disciminate models which possess $H^{\pm\pm}$. In section 4.1 and 4.2 we introduce the Higgs Triplet Model and Zee-Babu Model which may enhance both $\tau \to l_i l_j l_k$ and $\mu \to e\gamma$ to experimental observability by virtual exchange of $H_L^{\pm\pm}$ or $H_R^{\pm\pm}$. In section 4.3 we show how the P odd asymmetry for both decays may act as a powerful discriminator of the three models under consideration.

[3] For models with large extra dimensions see [34].

4.1 Higgs Triplet Model

In the Higgs Triplet Model (HTM) [35] a single $I = 1$, $Y = 2$ complex $SU(2)_L$ triplet is added to the SM. No right-handed neutrino is introduced, and the light neutrinos receive a Majorana mass proportional to the left-handed triplet vev (v_L) leading to the following neutrino mass matrix:

$$\mathcal{M}_\nu = \sqrt{2} v_L \begin{pmatrix} h_{ee} & h_{e\mu} & h_{e\tau} \\ h_{\mu e} & h_{\mu\mu} & h_{\mu\tau} \\ h_{\tau e} & h_{\tau\mu} & h_{\tau\tau} \end{pmatrix} . \tag{56}$$

In the HTM h_{ij} is directly related to the neutrino masses and mixing angles as follows:

$$h_{ij} = \frac{1}{\sqrt{2} v_L} V_{\text{MNS}} diag(m_1, m_2, m_3) V_{\text{MNS}}^T . \tag{57}$$

This expression for h_{ij} is essentially equivalent to that in CASE I with the replacements $(m_1, m_2, m_3) \to (M_1, M_2, M_3)$ and $v_L \to v_R$. In Eq.(57) v_L is a free parameter and is necessarily non-zero (unlike v_L in the LR symmetric model) in order to generate neutrino masses. Its magnitude may lie anywhere in the range eV $< v_L <$ 8 GeV, where the lower limit arises from the requirement of a perturbative h_{ij} satisfying Eq.(57) and the upper limit is derived from maintaining $\rho \sim 1$. In the HTM there is no $H_R^{\pm\pm}$ and so $\tau \to l_i l_j l_k$ is mediated solely by $H_L^{\pm\pm}$. Obtaining BR($\tau \to l_i l_j l_k$) $> 10^{-8}$ with $m_{H^{\pm\pm}} = 1$ TeV requires $|h^*_{\tau i} h_{jk}| > 10^{-3}$. Due to the ignorance of v_L the magnitude of h_{ij} cannot be predicted and so the HTM can only *accommodate* observable BRs for $\tau \to l_i l_j l_k$. However, unlike the LR symmetric model, the HTM provides predictions for the ratios of $\tau \to l_i l_j l_k$ [36] with are distinct for each of the various neutrino mass patterns NH, IH and DG. The necessary suppression of BR($\mu \to eee$) relative to BR($\tau \to lll$) requires $h_{e\mu}$ to be sufficiently small. As in CASE I Eq.(47), this is arranged by invoking a cancellation between two terms contributing to $h_{e\mu}$, one depending on θ_{13} and the other depending on both θ_{12} and $r = \Delta m^2_{12}/\Delta m^2_{13}$ [36],[37]. Observation of $\tau \to lll$ would restrict θ_{13} to a narrow interval which can be predicted in terms of θ_{12} and r. For the case of NH neutrinos $\theta_{13} \sim \sqrt{r}$ while for IH and DG neutrinos $\theta_{13} \sim r$. Since current oscillation data suggests $r \approx 0.04$, the value of θ_{13} need to ensure small $h_{e\mu}$ is of the order 0.1 for NH and 0.01 for IH and DG.

4.2 Two loop radiative singlet Higgs model (Zee-Babu model)

Neutrino mass may be absent at the tree-level but is generated radiatively via higher order diagrams involving $L = 2$ scalars. In the Zee-Babu model (ZBM) $SU(2)_L$ singlet charged scalars $H_R^{\pm\pm}$ and $H_L^{\pm}$ are added to the SM Lagrangian [38],[39] with the following Yukawa couplings:

$$\mathcal{L}_Y = f_{ij} \left(L^{Ta}_{iL} C L^b_{jL} \right) \epsilon_{ab} H_L^+ \; + \; h'_{ij} \left(l^T_{iR} C l_{jR} \right) H_R^{++} + h.c. \tag{58}$$

No right-handed neutrino is introduced. A Majorana mass for the light neutrinos arises at the two loop level in which the lepton number violating trilinear coupling $\mu H_L^\mp H_L^\mp H_R^{\pm\pm}$ plays a

crucial role. The explicit form for $\mathcal{M}_\nu$ is as follows:

$$\mathcal{M}_\nu = \zeta \times \begin{pmatrix} \epsilon^2\omega_{\tau\tau} + 2\epsilon\epsilon'\omega_{\mu\tau} + \epsilon'^2\omega_{\mu\mu} \ , & \epsilon\omega_{\tau\tau} + \epsilon'\omega_{\mu\tau} - \epsilon\epsilon'\omega_{e\tau} - \epsilon'^2\omega_{e\mu} \ , & -\epsilon\omega_{\tau\tau} - \epsilon'\omega_{\mu\mu} - \epsilon^2\omega_{e\tau} - \epsilon\epsilon'\omega_{e\mu} \\ . & \omega_{\tau\tau} - 2\epsilon'\omega_{e\tau} + \epsilon'^2\omega_{ee} \ , & -\omega_{\mu\tau} - \epsilon\omega_{e\tau} + \epsilon'\omega_{e\mu} + \epsilon\epsilon'\omega_{ee} \\ . & . & \omega_{\mu\mu} + 2\epsilon\omega_{e\mu} + \epsilon^2\omega_{ee} \end{pmatrix} , \tag{59}$$

where $\epsilon = f_{e\tau}/f_{\mu\tau}$, $\epsilon' = f_{e\mu}/f_{\mu\tau}$, $\omega_{ij} = h_{ij}m_i m_j$ (m_i, m_j are charged fermion masses), $h_{ij} = h'_{ij}(2h'_{ij})$ for $i = j$ ($i \neq j$) and ζ is given by:

$$\zeta = \frac{8\mu f_{\mu\tau}^2 \tilde{I}}{(16\pi^2)^2 m_{H^\pm}^2} \ . \tag{60}$$

Here $\tilde{I}$ is a dimensionless quantity of $\mathcal{O}(1)$ originating from the loop integration. Clearly the expression for $\mathcal{M}_\nu$ differs from that in the HTM and involves 9 arbitrary couplings. Since the model predicts one massless neutrino (at the two-loop level), quasi-degenerate neutrinos are not permitted (unlike the HTM) and only NH and IH mass patterns can be accommodated. The f couplings (contained in ϵ and ϵ') are directly related to the elements of $\mathcal{M}_\nu$. In the scenario of NH, $\epsilon \approx \epsilon' \approx \tan\theta_{12}/\sqrt{2}$ and $\sin\theta_{13}$ is close to zero. Since $\epsilon, \epsilon' < 1$ one may neglect those terms in $\mathcal{M}_\nu$ which are proportional to the electron mass (i.e. $\omega_{ee}, \omega_{e\mu}, \omega_{e\tau}$). This simplification leads to the following prediction [39]: $h_{\mu\mu} : h_{\mu\tau} : h_{\tau\tau} \approx 1 : m_\mu/m_\tau : (m_\mu/m_\tau)^2$. In the case of IH, large values are required for $\epsilon, \epsilon' (> 5)$, and thus neglecting $\omega_{ee}, \omega_{e\mu}, \omega_{e\tau}$ in $\mathcal{M}_\nu$ may not be entirely justified. However, if such terms are neglected [39] then the above prediction for the ratio of $h_{\mu\mu} : h_{\mu\tau} : h_{\tau\tau}$ also approximately holds for the case of IH. In the ZBM there is no $H_L^{\pm\pm}$ and so $\tau \to l_i l_j l_k$ is mediated solely by $H_R^{\pm\pm}$.

Another significant difference with the HTM is that eV scale neutrino masses requires f, $h_{\mu\mu} \sim 10^{-2}$, and thus LFV decays cannot be suppressed arbitrarily if the 2-loop diagram is solely responsible for the generation of the neutrino mass matrix. Such relatively large couplings are necessary since a rough upper bound on ζ (which is a function of model parameters) can be derived. In contrast, v_L in the HTM is arbitrary and eV scale neutrino masses can be accommodated even with $h_{ij} \sim 10^{-10}$. The requirement that f, $h_{\mu\mu} \sim 10^{-2}$ suggests that BR($\mu \to e\gamma$) and BR($\tau \to \mu\mu\mu$) could be within range of upcoming experiments [40].

Since h_{ee}, $h_{e\mu}$ and $h_{e\tau}$ may be treated as free parameters (essentially unrelated to the neutrino mass matrix) the necessary suppression of $\mu \to eee$ can be obtained by merely choosing $h_{e\mu}$ and/or h_{ee} very small. Observable rates for BR($\tau \to eee$) can be arranged by appropriate choice of h_{ee} and $h_{e\tau}$.

4.3 Sensitivity of P odd asymmetry to $H_L^{\pm\pm}$ and $H_R^{\pm\pm}$

Angular distributions of LFV decays can act as a powerful discriminator of models of new physics. The predictions for $\mu^+ \to e_L^+\gamma$ and $\mu^+ \to e_R^+\gamma$ depend on the chirality structure of LFV interactions and so in general would be model dependent. Ref.[41] defined various P odd and T odd asymmetries for $\mu \to e\gamma$ and $\mu \to eee$ and performed a numerical analysis in the context of supersymmetric $SU(5)$ and $SO(10)$. Analogous asymmetries were defined for

$\tau^\pm \to l^\pm\gamma$ and $\tau^\pm \to lll$ in [17]. In this section we apply the general formulae introduced in Refs.[17],[41] to the three models of interest which all contain $H^{\pm\pm}$.

For the decay $\mu^+ \to e^-e^+e^+$ with polarized μ^+, one defines θ_{e^-} as the angle between the polarization vector of μ^+ and the direction of the e^-, the latter taken to be the z direction. The P odd asymmetry $\mathcal{A}_P$ is defined as an asymmetry in the θ_{e^-} distribution. In contrast, for τ produced in the process $e^+e^- \to \tau^+\tau^-$ the helicity of the τ in the LFV decay $\tau \to lll$ is not known initially. Consequently, the experimental set up is sensitive to both $\tau_L^+ \to lll$ or $\tau_R^+ \to lll$. However, by exploiting the spin correlation of the pair produced τ (i.e. $e^+e^- \to \tau_L^+\tau_R^-, \tau_R^+\tau_L^-$) information on the helicity of the LFV decaying τ can be obtained by studying the angular and kinematical distributions of the non-LFV decay of the other τ in the $\tau \to lll$ event. For illustration we shall always take the non-LFV decay mode as $\tau \to \pi\nu$, although such an analysis can also be performed for other main decay modes such as $\tau \to \rho\nu, a_1\nu, l\nu\overline{\nu}$.

In the notation of [17] the effective 4-Fermi interaction for $\tau^+ \to \mu^-\mu^+\mu^+$ mediated by $H_{L,R}^{++}$ is as follows:

$$\mathcal{L} = \frac{-4G_F}{\sqrt{2}} \left\{ g_3(\overline{\tau}\gamma^\mu P_R\mu)(\overline{\mu}\gamma_\mu P_R\mu) + g_4(\overline{\tau}\gamma^\mu P_L\mu)(\overline{\mu}\gamma_\mu P_L\mu) \right\} \ . \tag{61}$$

The differential cross-section for the events $\tau^+ \to \mu^-\mu^+\mu^+$ (LFV) and $\tau^- \to \pi^-\nu$ (non-LFV) is:

$$\begin{aligned} & d\sigma(e^+e^- \to \tau^+\tau^- \to \mu^-\mu^+\mu^+ + \pi^-\nu) \\ & = \sigma(e^+e^- \to \tau^+\tau^-) BR(\tau^- \to \pi^-\nu) \left(\frac{m_\tau^5 G_{\rm F}^2}{128\pi^4}/\Gamma \right) \frac{d\cos\theta_\pi}{2} \ dx_1 \ dx_2 \ d\cos\theta \ d\phi \\ & \quad \times \left[X - \frac{s-2m_\tau^2}{s+2m_\tau^2} \left\{ Y \cos\theta \right\} \cos\theta_\pi \right] \ , \end{aligned} \tag{62}$$

where

$$X = (|g_3|^2 + |g_4|^2)\alpha_1(x_1, x_2); \ Y = (|g_3|^2 - |g_4|^2)\alpha_1(x_1, x_2) \ . \tag{63}$$

Here $\alpha_1(x_1, x_2)$ is a function of the energy variables $x_1 = 2E_1/m_\tau$ and $x_2 = 2E_2/m_\tau$ where $E_1(E_2)$ is the energy of μ^+ with larger (smaller) energy in the rest frame of τ^+:

$$\alpha_1(x_1, x_2) = 8(2 - x_1 - x_2)(x_1 + x_2 - 1) \ . \tag{64}$$

The angles θ and ϕ specify the decay plane of $\tau^+ \to \mu^-\mu^+\mu^+$ relative to the production plane of $e^+e^- \to \tau^+\tau^-$ in the τ^+ rest frame. The angle θ_π is the angle between the direction of momentum of τ^- and π^- in the τ^- rest frame. For a detailed discussion we refer the reader to [17]. It is clear that Y determines the angular dependence of Eq.(62) and thus Y is a measure of the P odd asymmetry for $\tau \to \mu\mu\mu$. For our quantitative study of its magnitude we define:

$$\mathcal{A}(\tau \to \mu\mu\mu) = \frac{|g_3|^2 - |g_4|^2}{|g_3|^2 + |g_4|^2} \ . \tag{65}$$

Clearly $\mathcal{A}(\tau \to \mu\mu\mu) = 0$ (± 1) corresponds to zero (maximal) asymmetry.

Table 2: Expressions for g_3, g_4 in the three models

	HTM ($H_L^{\pm\pm}$)	ZBM ($H_R^{\pm\pm}$)	LR ($H_{L,R}^{\pm\pm}$)
$-\frac{4G_F}{\sqrt{2}}g_3$	0	$\frac{h_{\mu\mu}h^*_{\tau\mu}}{M^2_{H_R^{\pm\pm}}}$	$\frac{h_{\mu\mu}h^*_{\tau\mu}}{M^2_{H_R^{\pm\pm}}}$
$-\frac{4G_F}{\sqrt{2}}g_4$	$\frac{h_{\mu\mu}h^*_{\tau\mu}}{M^2_{H_L^{\pm\pm}}}$	0	$\frac{h_{\mu\mu}h^*_{\tau\mu}}{M^2_{H_L^{\pm\pm}}}$

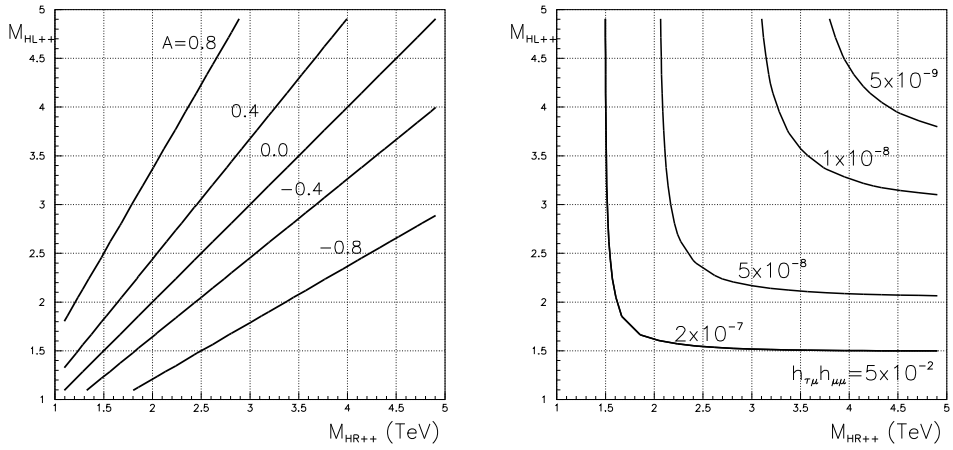

Figure 6: (a) $\mathcal{A}(\tau \to lll)$ and (b) BR$(\tau \to \mu\mu\mu)$ and in the plane ($M_{H_L^{\pm\pm}}$, $M_{H_R^{\pm\pm}}$)

The expressions for g_3 and g_4 in the three models under consideration are given in Table 2. In the manifest LR symmetric model h_{ij} cancels out in the expression for $\mathcal{A}(\tau \to lll)$ leaving a simple dependence on $M_{H_L^{\pm\pm}}$ and $M_{H_R^{\pm\pm}}$ which applies to all six $\tau \to lll$ decays:

$$\mathcal{A}(\tau \to lll) = \frac{1/M^4_{H_R^{\pm\pm}} - 1/M^4_{H_L^{\pm\pm}}}{1/M^4_{H_R^{\pm\pm}} + 1/M^4_{H_L^{\pm\pm}}} \ . \tag{66}$$

In Fig.6 (a) $\mathcal{A}(\tau \to lll)$ in plotted in the plane $(M_{H_L^{\pm\pm}}, M_{H_R^{\pm\pm}})$. Clearly the case of degeneracy ($M_{H_L^{\pm\pm}} = M_{H_R^{\pm\pm}}$) gives $\mathcal{A}(\tau \to lll) = 0$, while $M_{H_L^{\pm\pm}} > M_{H_R^{\pm\pm}}$ ($M_{H_L^{\pm\pm}} < M_{H_R^{\pm\pm}}$) results in positive (negative) $\mathcal{A}(\tau \to lll)$. For the HTM and ZBM the asymmetry is maximal, being -1 and $+1$ respectively. Consequently, $\mathcal{A}(\tau \to lll)$ in the LR symmetric model may differ significantly from the corresponding value in models with only a $H_L^{\pm\pm}$ (HTM) or $H_R^{\pm\pm}$ (ZBM). Thus $\mathcal{A}(\tau \to lll)$ has the potential to discriminate between the various models with a $H^{\pm\pm}$. In addition, in the context of the LR model a measurement of $\mathcal{A}(\tau \to lll)$ provides important information on the ratio $M_{H_L^{\pm\pm}}/M_{H_R^{\pm\pm}}$, which could assist the direct searches for $H_L^{\pm\pm}$ and $H_R^{\pm\pm}$ at high energy colliders. For comparison we show in Fig.6 (b) the dependence of BR$(\tau \to \mu\mu\mu)$ on $M_{H_L^{\pm\pm}}$ and $M_{H_R^{\pm\pm}}$ for $|h_{\mu\mu}h^*_{\tau\mu}| = 0.05$.

Of the order of 50 $\tau \to lll$ events would be needed to distinguish $\mathcal{A}(\tau \to lll) = +1$ from -1. A high luminosity upgrade of the existing B factories anticipates up 10^{10} $\tau^+\tau^-$ pairs and thus $\mathrm{BR}(\tau \to lll) > 10^{-8}$ would allow measurements of $\mathcal{A}(\tau \to lll)$. From Fig.6 (a) it is clear that a LR model with $M_{H_L^{\pm\pm}} \ll M_{H_R^{\pm\pm}}$ ($M_{H_R^{\pm\pm}} \ll M_{H_L^{\pm\pm}}$) will give an almost maximal $\mathcal{A}(\tau \to lll)$ and consequently would be difficult to distinguish from the HTM (ZBM). However, if a signal were also observed for $\mu^+ \to e^+\gamma$, the analogous P odd asymmetry, $\mathcal{A}(\mu \to e\gamma)$, can serve as an additional discriminator:

$$\mathcal{A}(\mu \to e\gamma) = \frac{|A_L|^2 - |A_R|^2}{|A_L|^2 + |A_R|^2} \ . \tag{67}$$

In CASE I, Fig.3 there is a parameter space for $\mathrm{BR}(\tau \to \mu\mu\mu) \approx 10^{-8}$ and $\mathrm{BR}(\mu \to e\gamma) \approx 10^{-12}$), which might provide sufficient events for both asymmetries to be measured. In contrast to $\tau \to \mu\mu\mu$, the loop induced decay $\mu \to e\gamma$ can be mediated by $H_{L,R}^{\pm\pm}$, $H_1^\pm$ and $W_R^\pm$ in the LR symmetric model. One may write a simplified formula for A_L and A_R (written explicitly in Eqs. (28) and (30)), where a, b, c, d are functions of masses and the heavy neutrino mixing matrix K_R:

$$\begin{aligned} A_L &= a\ (M_{H_R^{\pm\pm}}, K_R) + b\ (M_{W_R^\pm}, K_R, M_i)\ , \\ A_R &= c\ (M_{H_L^{\pm\pm}}, K_R) + d\ (M_{H_1^\pm}, K_R)\ . \end{aligned} \tag{68}$$

In the LR model usually $a, c \gg b, d$ and so the dominant contribution to $\mathcal{A}(\mu \to e\gamma)$ arises from $H_L^{\pm\pm}$ and $H_R^{\pm\pm}$. Hence in LR models one expects $\mathcal{A}(\mu \to e\gamma) \sim \mathcal{A}(\tau \to lll)$. This is shown in Fig.7 where $\mathcal{A}(\tau \to \mu\mu\mu)$ is plotted against $\mathcal{A}(\mu \to e\gamma)$ for CASE I with $\sin\theta_{13} = 0.2$ and $\delta = \pi$. The plotted points correspond to observable rates for both LFV decays (taken to be $10^{-9} \leq \mathrm{BR}(\tau \to \mu\mu\mu) \leq 10^{-7}$ and $10^{-14} \leq \mathrm{BR}(\mu \to e\gamma) \leq 10^{-11}$), within the following parameter region: $M_{W_2} = 3$ TeV, 1 TeV $\leq M_i \leq 5$ TeV, 2 TeV $\leq M_{H_L^{\pm\pm}} = M_{H_1^\pm} \neq M_{H_R^{\pm\pm}} \leq 4$ TeV. Each point also satisfies the constraint $\mathrm{BR}(\mu \to eee) < 10^{-12}$. Clearly the vast majority of the points are close to the line $\mathcal{A}(\mu \to e\gamma) = \mathcal{A}(\tau \to lll)$, showing that the diagrams involving $H_L^{\pm\pm}$ and $H_R^{\pm\pm}$ give the dominant contribution over most of the parameter space. The asymmetries differ sizeably only when M_i and M_{W_R} are considerably smaller than $M_{H_L^{\pm\pm}}$ and $M_{H_R^{\pm\pm}}$. In the HTM one has:

$$\begin{aligned} A_L &= 0\ , \\ A_R &= c\ (M_{H_L^{\pm\pm}}, h_{ij}) + d\ (M_{H_L^\pm}, h_{ij})\ . \end{aligned} \tag{69}$$

and thus $\mathcal{A}(\mu \to e\gamma)$ is maximal. In the ZBM:

$$\begin{aligned} A_L &= a\ (M_{H_R^{\pm\pm}}, h_{ij})\ , \\ A_R &= d\ (M_{H_L^\pm}, f_{ij})\ . \end{aligned} \tag{70}$$

$\mathcal{A}(\mu \to e\gamma)$ may take any value since the masses of $H_L^\pm$ and $H_R^{\pm\pm}$ are unrelated and $h_{ij} \neq f_{ij}$ in general. The allowed ranges of $\mathcal{A}(\tau \to lll)$ and $\mathcal{A}(\mu \to e\gamma)$ in the three models under consideration are summarized in Table 3. It is clear that if signals for both $\tau \to lll$ and $\mu \to e\gamma$ are observed, the corresponding asymmetries may act as a powerful discriminator of the models.

Table 3: P odd asymmetries $\mathcal{A}(\tau \to lll)$ and $\mathcal{A}(\mu \to e\gamma)$ in the three models

	HTM ($H_L^{\pm\pm}$)	ZBM ($H_R^{\pm\pm}$)	LR ($H_{L,R}^{\pm\pm}$)
$\mathcal{A}(\mu \to e\gamma)$	-1	$-1 < \mathcal{A} < +1$	$-1 < \mathcal{A} < +1$
$\mathcal{A}(\tau \to lll)$	-1	$+1$	$-1 < \mathcal{A} < +1$

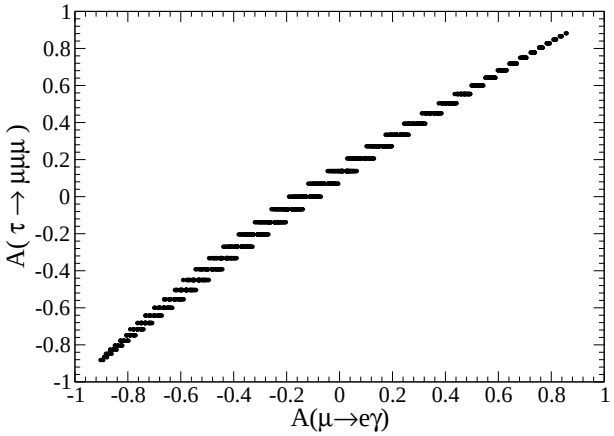

Figure 7: Correlation between $\mathcal{A}(\mu \to e\gamma)$ and $\mathcal{A}(\tau \to \mu\mu\mu)$ in the LR model.

5 Conclusions

The Left-Right symmetric extension of the Standard Model with TeV scale breaking of $SU(2)_R$ via a right handed Higgs isospin triplet vacuum expectation value provides an attractive explanation for neutrino masses via the seesaw mechanism. The doubly charged scalars $H_L^{\pm\pm}$ and $H_R^{\pm\pm}$ with mass of order TeV mediate the LFV decays $\tau \to lll$ at tree-level via a Yukawa coupling h_{ij} which is related to the Maki-Nakagawa-Sakata matrix ($V_{\rm MNS}$). We introduced four ansatz for the origin of the bi-large mixing in $V_{\rm MNS}$ which satisfy the stringent bound $\mathrm{BR}(\mu \to eee) < 10^{-12}$ in distinct ways. A numerical study of the magnitude and correlation of $\mathrm{BR}(\tau^\pm \to lll)$ and $\mathrm{BR}(\mu \to e\gamma)$ was performed. It was shown that the number of observable rates for such LFV decays depends sensitively on the origin of the bi-large mixing in $V_{\rm MNS}$, with multiple LFV signals being possible in specific cases.

If a signal for $\tau \to lll$ were observed we showed how the definition of an angular asymmetry provides information on the relative strength of the contributions from $H_L^{\pm\pm}$ and $H_R^{\pm\pm}$. Such an asymmetry may also be used to distinguish the LR symmetric model from other models which contain either $H_L^{\pm\pm}$ or $H_R^{\pm\pm}$ and thus predict maximal asymmetries.

Acknowledgements

Y.O was supported in part by the Grant-in-Aid for Science Research, Ministry of Education, Science and Culture, Nos. 16081211, 13135225 and 17540286. A.G.A was supported by National Cheng Kung University grant OUA 95-3-2-057.

References

[1] Y. Fukuda *et al.* [Super-Kamiokande Collaboration], Phys. Rev. Lett. **81**, 1562 (1998).

[2] Y. Kuno and Y. Okada, Rev. Mod. Phys. **73**, 151 (2001).

[3] P. Minkowski, Phys. Lett. B **67**, 421 (1977); T. Yanagida, in *Proceedings of the Workshop on Unified Theory and Baryon Number of the Universe*, edited by O. Sawada and A. Sugamoto (KEK, 1979) p.95; M. Gell-Mann, P. Ramond, and R. Slansky, in *Supergravity*, edited by P. van Nieuwenhuizen and D. Freedman (North Holland, Amsterdam, 1979).

[4] J. C. Pati and A. Salam, Phys. Rev. D **10**, 275 (1974); R. N. Mohapatra and J. C. Pati, Phys. Rev. D **11**, 2558 (1975). G. Senjanovic and R. N. Mohapatra, Phys. Rev. D **12**, 1502 (1975).

[5] R. N. Mohapatra and G. Senjanovic, Phys. Rev. Lett. **44**, 912 (1980).

[6] J. F. Gunion, J. Grifols, A. Mendez, B. Kayser and F. I. Olness, Phys. Rev. D **40**, 1546 (1989).

[7] N. G. Deshpande, J. F. Gunion, B. Kayser and F. I. Olness, Phys. Rev. D **44**, 837 (1991).

[8] M. L. Swartz, Phys. Rev. D **40**, 1521 (1989).

[9] V. Cirigliano, A. Kurylov, M. J. Ramsey-Musolf and P. Vogel, Phys. Rev. D **70**, 075007 (2004).

[10] M. Grassi [MEG Collaboration], Nucl. Phys. Proc. Suppl. **149**, 369 (2005).

[11] Y. Yusa *et al.* [Belle Collaboration], Phys. Lett. B **589**, 103 (2004).

[12] B. Aubert *et al.* [BABAR Collaboration], Phys. Rev. Lett. **92**, 121801 (2004).

[13] S. Hashimoto *et al.*, "Letter of intent for KEK Super B Factory," KEK-REPORT-2004-4; A. G. Akeroyd *et al.* [SuperKEKB Physics Working Group], arXiv:hep-ex/0406071.

[14] R. Santinelli, eConf **C0209101**, WE14 (2002) [Nucl. Phys. Proc. Suppl. **123**, 234 (2003)] [arXiv:hep-ex/0210033].

[15] A. Dedes, J. R. Ellis and M. Raidal, Phys. Lett. B **549**, 159 (2002); K. S. Babu and C. Kolda, Phys. Rev. Lett. **89**, 241802 (2002); G. Cvetic, C. Dib, C. S. Kim and J. D. Kim, Phys. Rev. D **66**, 034008 (2002) [Erratum-ibid. D **68**, 059901 (2003)]; A. Brignole and A. Rossi, Phys. Lett. B **566**, 217 (2003); Y. F. Zhou, J. Phys. G **30**, 783 (2004); S. Kanemura, T. Ota and K. Tsumura, Phys. Rev. D **73**, 016006 (2006); P. Paradisi, JHEP **0602**, 050 (2006); E. Arganda and M. J. Herrero, Phys. Rev. D **73**, 055003 (2006); C. H. Chen and C. Q. Geng, Phys. Rev. D **74**, 035010 (2006).

[16] U. Bellgardt *et al.* [SINDRUM Collaboration], Nucl. Phys. B **299**, 1 (1988).

[17] R. Kitano and Y. Okada, Phys. Rev. D **63**, 113003 (2001).

[18] J. F. Gunion, C. Loomis and K. T. Pitts, eConf **C960625**, LTH096 (1996) [arXiv:hep-ph/9610237]; K. Huitu, J. Maalampi, A. Pietila and M. Raidal, Nucl. Phys. B **487**, 27 (1997); J. Maalampi and N. Romanenko, Phys. Lett. B **532**, 202 (2002); G. Azuelos, K. Benslama and J. Ferland, J. Phys. G **32**, 73 (2006); A. G. Akeroyd and M. Aoki, Phys. Rev. D **72**, 035011 (2005).

[19] Z. Maki, M. Nakagawa and S. Sakata, Prog. Theor. Phys. **28**, 870 (1962).

[20] P. Duka, J. Gluza and M. Zralek, Annals Phys. **280**, 336 (2000).

[21] K. Kiers, M. Assis, D. Simons, A. A. Petrov and A. Soni, Phys. Rev. D **73**, 033009 (2006).

[22] F. Cuypers and S. Davidson, Eur. Phys. J. C **2**, 503 (1998); O. M. Boyarkin, G. G. Boyarkina and T. I. Bakanova, Phys. Rev. D **70**, 113010 (2004).

[23] B. Aharmim *et al.* [SNO Collaboration], Phys. Rev. C **72**, 055502 (2005).

[24] T. Araki *et al.* [KamLAND Collaboration], Phys. Rev. Lett. **94**, 081801 (2005).

[25] Y. Ashie *et al.* [Super-Kamiokande Collaboration], Phys. Rev. D **71**, 112005 (2005).

[26] E. Aliu *et al.* [K2K Collaboration], Phys. Rev. Lett. **94**, 081802 (2005).

[27] M. Apollonio *et al.* [CHOOZ Collaboration], Eur. Phys. J. C **27**, 331 (2003).

[28] F. Boehm *et al.*, Phys. Rev. D **64**, 112001 (2001).

[29] D. N. Spergel *et al.*, arXiv:astro-ph/0603449.

[30] J. A. Casas and A. Ibarra, Nucl. Phys. B **618**, 171 (2001); J. R. Ellis, J. Hisano, M. Raidal and Y. Shimizu, Phys. Rev. D **66**, 115013 (2002).

[31] W. M. Yao *et al.* [Particle Data Group], J. Phys. G **33**, 1 (2006).

[32] A. Czarnecki and E. Jankowski, Phys. Rev. D **65**, 113004 (2002).

[33] R. N. Mohapatra, Phys. Rev. D **34**, 909 (1986).

[34] W. F. Chang and J. N. Ng, Phys. Rev. D **71**, 053003 (2005).

[35] J. Schechter and J. W. F. Valle, Phys. Rev. D **22**, 2227 (1980); G. B. Gelmini and M. Roncadelli, Phys. Lett. B **99**, 411 (1981).

[36] E. J. Chun, K. Y. Lee and S. C. Park, Phys. Lett. B **566**, 142 (2003).

[37] M. Kakizaki, Y. Ogura and F. Shima, Phys. Lett. B **566**, 210 (2003).

[38] A. Zee, Nucl. Phys. B **264**, 99 (1986); K. S. Babu, Phys. Lett. B **203**, 132 (1988).

[39] K. S. Babu and C. Macesanu, Phys. Rev. D **67**, 073010 (2003).

[40] D. A. Sierra and M. Hirsch, arXiv:hep-ph/0609307.

[41] Y. Okada, K. i. Okumura and Y. Shimizu, Phys. Rev. D **61**, 094001 (2000).